J Solid State Electrochem (2012) 16:681–687
DOI 10.1007/s10008-011-1385-9

ORIGINAL PAPER

Self-assembled architecture based on triiron-substituted polyoxomolybdate anion and positively charged polymer

Graziella Turdean · Ionel Catalin Popescu

Received: 24 January 2011 / Revised: 16 March 2011 / Accepted: 17 March 2011 / Published online: 6 May 2011
© Springer-Verlag 2011

Abstract A new self-assembled multilayer architecture was constructed by successive deposition of poly(4-vinylpyridine) partially quaternized with ethylamine (B) and Keggin trilacunary polyoxomolybdate $[A\alpha\text{-}PFe_3^{III}(H_2O)_3Mo_9O_{37}]^{6-}$ (PFe_3Mo_9) on the Au electrode surface, covered with 3-mercapto-1-propanesulfonic acid (MPS). Surface plasmon resonance and cyclic voltammetry measurements were performed at Au/MPS/B/PFe_3Mo_9/B interface in order to investigate the structure and the electrochemical behavior of this electrode. Due to the presence of PFe_3Mo_9, the Au/MPS/B/PFe_3Mo_9/B-modified electrode showed electrocatalytic activity towards H_2O_2 amperometric detection. Additionally, when GOx was deposited as the outermost layer on the abovementioned multilayer structure, the Au/MPS/B/PFe_3Mo_9/B/GOx-modified electrode was able to detect glucose.

Keywords Self-assembled architecture · Polyoxometallates · Amperometric sensor/biosensor · Hydrogen peroxide · Glucose oxidase

Introduction

Polyoxometallates and especially Keggin type complexes containing transition metals are interesting electrocatalysts because of their ability to: (1) adsorb on various conventional electrode materials; (2) undergo stepwise reversible multi-electron transfers; (3) exhibit tunable redox and acid–base properties by coherent changes of their chemical composition; (4) show high stability in acidic media; (5) participate at fast inner-sphere electron-transfer reactions [1–7].

The transition metal-substituted polyoxometallates were frequently investigated for their remarkable electrocatalytic properties, in view to detect chemical species of practical importance, such as H_2O_2, NO_2^-, BrO_3^-, etc. Among these, Fe(III)-substituted polyoxometallates with Keggin [5–9], Dawson [10, 11], or sandwich-type structures [12, 13] were found of particular interest.

In order to obtain efficient modified electrodes, the polyoxometallates were immobilized on the surface of different electrode materials by using various methods, such as irreversible adsorption [9, 14–16], electrodeposition [14, 16, 17], sol–gel approach [14], entrapping into conducting polymers [5, 14, 18], and self-assembling based on electrostatic interactions between oppositely charged species [14, 19–23].

Nowadays, the self-assembling approach is considered a central way to prepare modified electrodes with important advantages, such as: (1) the possibility to design the architecture deposited on electrode surface, aiming to obtain electrochemical systems with specific properties; (2) the ordered molecular structure allows optimizing the molecular or supramolecular interactions; (3) the entire electrode surface exhibits a cooperative and homogenous behavior; (4) the undesired accumulation of species close to the electrode surface is avoided or, at least, decreased [24]. Consequently, the self-assembling method has been applied to build up, on the surface of various electrode materials, a variety of mono- or multilayer architectures incorporating various polyoxometallates, such as $AsMo_{11}VO_{40}^{4-}$ [4], $H_4PW_{18}O_{62}^{7-}$ [25], PMo_{12} [14, 21], $SiW_{11}O_{39}Fe(H_2O)^{6-}$ [9], $SiMo_{11}VO_{40}^{5-}$ [16, 19, 20], $SiW_{12}O_{40}^{4-}$ [22], and $BW_{12}O_{40}^{5-}$ [23]. In this context, it is worth to mention that basically two strategies were used to obtain modified electrodes based on self-

G. Turdean (✉) · I. C. Popescu
Department of Physical Chemistry, University "Babes-Bolyai", RO-400028, Cluj-Napoca, Romania
e-mail: gturdean@chem.ubbcluj.ro

assembled architectures films incorporating polyoxometallates: the immersion growth [4, 9, 14, 16, 19, 21–23, 25] and the electrochemical growth [16, 20]. In spite of the great variety resulting from the combination of these techniques and different polyoxometallates, only few modified electrodes exploiting layer-by-layer deposition [14, 19, 21, 25] and spontaneous adsorption [9] techniques, showed interesting electrocatalytic properties for the amperometric detection of NO_2^- [9, 19, 25], BrO_3^- [14, 19, 21], and H_2O_2 [9].

Taking into account, the good electrocatalytic activity of a new Keggin trilacunary polyoxomolybdate, $[A\alpha\text{-}PFe_3^{III}(H_2O)_3Mo_9O_{37}]^{6-}$ (PFe_3Mo_9), evidenced in the case of H_2O_2 homogenous reduction of [8] and the simplicity and versatility of the immersion growth strategy, a new self-assembled multilayer architecture for H_2O_2 electrocatalytic reduction was deposited on the Au electrode surface covered with 3-mercapto-1-propanesulfonic acid (MPS) by using the layer-by-layer deposition of a positively charged polymer, poly(4-vinylpyridine) partially quaternized with ethylamine (B) and PFe_3Mo_9. In order to investigate the structure of the built-up architecture, as well as its functionality, cyclic voltammetry and surface plasmon resonance (SPR) measurements were performed under different experimental conditions (different potential scan rates and various compositions of the surrounding electrolyte) at the Au/MPS/B/PFe_3Mo_9/B-modified electrode. Finally, by immobilizing negatively charged glucose oxidase (with the isoelectric point of 4.2) as outermost layer on Au/MPS/B/PFe_3Mo_9/B electrode, a new bioelectrode for glucose detection was obtained and characterized. To the best of our knowledge, we report here the first example of using the immersion growth technique to obtain modified electrodes incorporating an Fe(III)-substituted polyoxometallate as electrocatalyst for H_2O_2 and glucose amperometric detection. Thus, the electrode sensitivity can be controlled by increasing the electrocatalyst concentration in the built-up architecture.

Experimental

Chemicals

The trilacunary Keggin type $Na_3H_3[A\alpha\text{-}PFe_3^{III}(H_2O)_3\text{-}Mo_9O_{37}]$ *14 H_2O (PFe_3Mo_9) complex was prepared as described elsewhere [8] and was used without any further purification. The PFe_3Mo_9 solutions were freshly prepared just before use, by dissolving the appropriate amounts of complex into the supporting electrolyte.

The supporting electrolyte was 0.4 M solution of Na_2SO_4, prepared from the corresponding salt provided by Merck (Darmstadt, Germany). The pH values of the supporting electrolyte were adjusted in the pH range 5.5–7 by adding 1/15 M phosphate buffer and in the pH range 1–5.5 by using diluted sulfuric acid. The 1/15 M phosphate buffer (pH 7) was obtained by mixing the appropriate volumes of Na_2HPO_4*12 H_2O and KH_2PO_4 solutions, prepared from the corresponding salts purchased from Merck. The sodium salt of 3-mercapto-1-propanesulfonic acid (MPS) and glucose oxydase (GOx) from *Aspergillus niger* (EC 1.1.3.4, type VII-S) were purchased from Sigma-Aldrich (St. Louis, MO, USA). The positively charged polymer, poly(4-vinylpyridine) partially quaternized with ethylamine (B), was received from Prof. E. Dominquez (Department of Analytical Chemistry, University of Alcalá de Henares, Spain). The D(−) glucose and hydrogen peroxide (30%) were obtained from Fluka (Sigma-Aldrich) and Merck, respectively. All other chemicals used (KOH, H_2SO_4 98%, HNO_3 60%, ethanol 98%) were of analytical grade and were purchased from Merck. The deionised water was obtained by using the Millipore Milli-Q system.

Preparation of the Au/MPS/B/PFe_3Mo_9/B-modified electrode

Gold wires (99.99% purity) of 0.5 mm diameter (geometrical area ~0.16 cm^2) were obtained from Goodfellow Cambridge (Huntingdon, England). The Au wire electrodes, were treated with a mixture of "piranha" solution (98% H_2SO_4 and 30% H_2O_2, 7:3 *v/v. Caution: piranha solution is corrosive and reacts violently with organic compounds; suitable precautions must be taken at all times*) for 30 min, rinsed in water, and, finally, boiled in a saturated KOH solution for 2 h. The cleaned wire electrodes were stored in concentrated H_2SO_4. Prior to use, the cleaned gold electrodes were dipped into a 60% HNO_3 solution for 10 min and then were thoroughly rinsed with distilled water. The negatively charged gold electrode surface (Au/MPS) was obtained by immersion of the cleaned Au wire into a 1 mM ethanolic solution of MPS for 12 h, followed by rinsing with ethanol.

The Au/MPS/B/PFe_3Mo_9/B self-assembled architecture was built up by sequential deposition of B, PFe_3Mo_9, and again B, by using the alternate immersion of Au/MPS electrode into the corresponding solution (10 mg of B/L in water or 3×10^{-3} M of PFe_3Mo_9 in 0.4 M Na_2SO_4) at room temperature, under vigorous stirring [26–30]. In all cases, the adsorption time was 2 h.

Preparation of the Au/MPS/B/PFe_3Mo_9/B/GOx-modified electrode

In order to obtain the amperometric transducer for glucose detection, GOx was immobilized as the outmost layer on Au/MPS/B/PFe_3Mo_9/B, by self-deposition (2 h under continuous stirring) from an aqueous solution containing 1 mg of GOx/mL (pH 6.6).

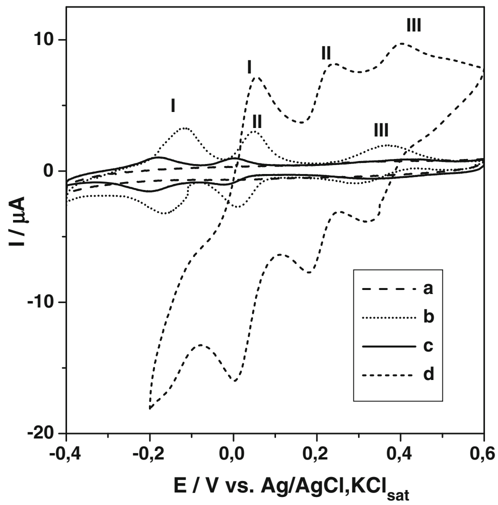

Fig. 1 Cyclic voltammetric response recorded at different modified electrodes: **a** Au/MPS/B; **b** Au/MPS/B/PFe_3Mo_9; **c** Au/MPS/B/PFe_3Mo_9/B/GOx; **d** Au//10^{-3} M PFe_3Mo_9. Experimental conditions: supporting electrolyte, 0.4 M Na_2SO_4 [pH 6.2 (**a**–**c**) and pH 2.5 (**d**)]; scan rate, 100 mV/s (**a**–**c**) and 25 mV/s (**d**), starting potential, −0.4 V vs. Ag/AgCl,KCl_{sat} (**a**–**c**) and −0.25 V vs. Ag/AgCl,KCl_{sat} (**d**)

SPR measurements

The BIACORE X^{TM} instrument (*BIAcore AB, Sweden*) was used for SPR measurements. In order to build up on the plain surface of the SPR gold chip (J1 PIONNER), the same architecture as that used for electrochemical experiments, a similar protocol to that above described was used. Thus, in a first step, the gold surface was cleaned using the "piranha" solution and then it was modified with MPS. Furthermore, the Au/MPS/$(B/PFe_3Mo_9)_n$/B and Au/MPS/B/PFe_3Mo_9/B/GOx architectures were step-by-step constructed by injecting, successively, 30 μL of appropriate aqueous solutions containing: (1) 25 mg of B/L; (2) 3 mM PFe_3Mo_9 and 0.4 M Na_2SO_4; (3) 1 mg GOx/mL. The variation of the SPR signal was continuously monitored and the steady-state values corresponding for different built architectures were recorded. For all SPR experiments, MilliQ water was used as flow carrier (flow rate of 20 μL min^{-1} and 25 °C).

Electrochemical measurements

Cyclic voltammograms and batch amperometric measurements were carried out in a conventional three-electrode electrochemical cell, connected to a voltammetric analyzer (PGSTAT 10, EcoChemie, Netherlands) controlled by a personal computer. The potential of the working electrode (Au-modified electrodes) was measured against Ag/AgCl, KCl_{sat} as reference electrode (Radiometer, France). A Pt plate was used as counter electrode. In order to obtain the calibration curve for H_2O_2 at Au/MPS/B/PFe_3Mo_9 modified electrode, amperometric measurements were performed at an applied potential of −0.1 V vs. Ag/AgCl,KCl_{sat}, in magnetically stirred solutions (500 rpm), at room temperature.

Results and discussions

Electrochemical and SPR characterization of the multilayer architecture

As expected, when the structure of the electrochemical interface was changed from Au or graphite [8], naked electrodes to Au/MPS/B/PFe_3Mo_9 or Au/MPS/B/PFe_3Mo_9/B/GOx-modified electrodes, the redox behavior of PFe_3Mo_9 was not significantly affected. Indeed, irrespective the nature of the modified electrode, the voltammetric response of PFe_3Mo_9 incorporated in both multilayer structures mentioned above shows three peak pairs (Fig. 1), each one involving a quasi-reversible transfer of $2e^-$ [8]. This invariance of the voltammetric response, observed for the immobilized PFe_3Mo_9, proves that the polyoxomolybdate anion remains electrically connected to the Au electrode in both investigated structures.

As a first step on the route to obtain the Au/MPS/B/PFe_3Mo_9-modified electrode, the absence of any redox activity characteristic to Au electrode, evidenced by the

Table 1 Electrochemical parameters of Au/MPS/B/PFe_3Mo_9 and Au/MPS/B/PFe_3Mo_9/B/GOx-modified electrodes

Electrode	Peak pairs	$E^{\varnothing\prime}$ V vs. Ag/AgCl,KCl_{sat}	ΔE_p	$I_{p,a}/I_{p,c}$
Au//10^{-3} M PFe_3Mo_9	I	0.030	0.052	1.05
	II	0.210	0.055	0.92
	III	0.360	0.077	0.65
Au/MPS/B/PFe_3Mo_9	I	−0.145	0.056	1.31
	II	+0.030	0.040	1.10
	III	+0.331	0.078	1.52
Au/MPS/B/PFe_3Mo_9/B/GOx	I	−0.190	0.018	1.16
	II	−0.010	0.020	1.26
	III	+0.377	0.097	0.68

$E^{\varnothing\prime}$ stands for the formal standard potential, calculated as mean of the anodic and cathodic peak potentials; ΔE_p stands for the potential peaks separation cyclic voltammogram recorded at Au/MPS/B-modified electrode (curve a, Fig. 1), confirms that whole Au surface was covered by the self-assembled MPS/B layer. Then, comparing the voltammetric response of the Au/MPS/B/ PFe_3Mo_9-modified electrode (curve b, Fig. 1) with that recorded for dissolved PFe_3Mo_9 at naked Au electrode (curve d, Fig. 1), it can be seen that I and II peak pairs were shifted towards negative potentials (Table 1). Taking into account that dissolved PFe_3Mo_9 exhibited at naked Au electrode a similar behavior with that observed at naked graphite electrode [8], the observed negative shift (175 mV for peak pair I; 180 mV for peak pair II) should be due to the attractive electrostatic interactions existing between the positively charged surface of Au/MPS/B electrode and the immobilized polyoxomolybdate anion.

Moreover, it is interesting to notice that III peak pair (placed at the most positive potentials), which was reported to be an overlap of $Fe^{3+/2+}$ and oxocage responses [8], was less affected by the change of bare Au surface ($E^{\varnothing\prime}_{III}$=0.331 V vs. Ag/AgCl,$KCl_{sat}$) with Au/MPS/B interface ($E^{\varnothing\prime}_{III}$=0.376 V vs. Ag/AgCl,$KCl_{sat}$). At the same time, it should be noticed that the peak currents corresponding to the Au/MPS/B/ PFe_3Mo_9 electrode were significantly lower than those recorded for dissolved PFe_3Mo_9 at naked Au electrode. This is probably due to a lower surface concentration of the immobilized polyoxomolybdate anion, and/or a larger distance between its redox centers and the electrode surface.

When GOx was immobilized on the top of MPS/B/ PFe_3Mo_9/B multilayer structure, the resulting modified electrode still displays the redox characteristics of PFe_3Mo_9 (Fig. 1, curve b). However, the peaks' intensities observed at Au/MPS/B/PFe_3Mo_9/B/GOx electrode (see curve c, Fig. 1) were much lower compared with those corresponding to Au/ MPS/B/PFe_3Mo_9 electrode (see curve b, Fig. 1), probably due to the expected permeability decrease of the multilayer structure and/or to inherent loss of PFe_3Mo_9 during the construction of Au/MPS/B/PFe_3Mo_9/B/GOx-modified electrode. Additionally, the GOx presence induces a shift towards negative potentials of both I and II peaks pairs (45 mV for I; 40 mV for II) (Table 1). This behavior can be explained observing that in Au/MPS/B/PFe_3Mo_9/B/GOx structure PFe_3Mo_9 is surrounded by two positively charged polymer layers (B) (Fig. 1, curve c), while only one layer of B is present in Au/MPS/B/PFe_3Mo_9 structure (Fig. 1, curve b).

It is worth to mention, that the reversibility of the redox processes (expressed by ΔE_p and $I_{p,a}/I_{p,c}$ parameters), involved in the voltammetric response of PFe_3Mo_9 at bare Au and Au/MPS/B/PFe_3Mo_9 electrodes, is roughly the same, irrespective of the nature of the electrochemical interface (Table 1). At the same time, all ΔE_p values were

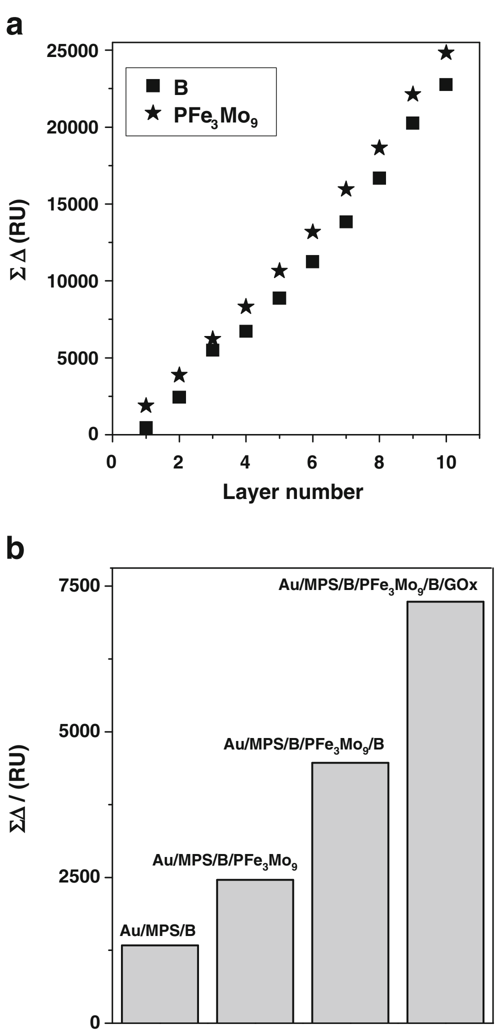

Fig. 2 Cumulative variation of the steady-state SPR response recorded for the architectures builded successively on Au/MPS surface: Au/MPS/ $(B/PFe_3Mo_9)_n$/B (**a**) and Au/MPS/B/PFe_3Mo_9/B/GOx (**b**). SPR results were expressed in relative units (*RU*)

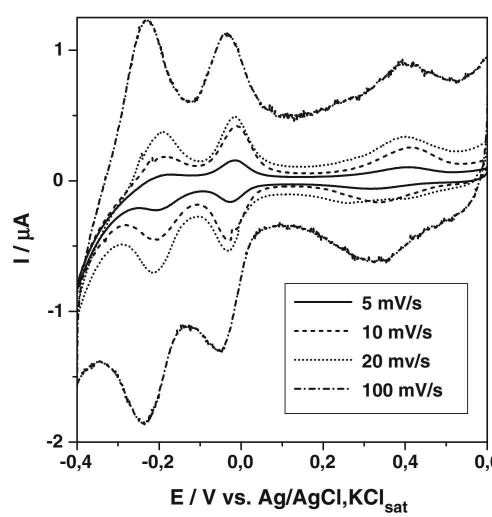

Fig. 3 The influence of the potential scan rate on the voltammetric behavior of Au/MPS/B/PFe_3Mo_9/B/GOx electrode. Experimental conditions: supporting electrolyte, 0.4 M Na_2SO_4 (pH 6.2); starting potential, −0.4 V vs. Ag/AgCl,KCl_{sat}

higher than the value expected for a surface-confined redox couple [31]. This could be due to the local non-equivalence of the redox centers [32] and/or to the local interactions between them [33]. Concerning the Au/MPS/B/PFe_3Mo_9/B/GOx electrode, the decrease of the ΔE_p values, observed for the peak pairs I and II (Table 1), suggest the reversibility increase of the redox processes involved in these peak generation. This effect could be the result of PFe_3Mo_9 intercalation between the layers of positively charged polymer (B).

Taking into account that SPR technique is able to monitor small changes in the refractive index at Au-solution interface, induced by adsorption of various molecules or biomolecules [34–37], SPR measurements were used to investigate the building process of the MPS/B/PFe_3Mo_9/B/GOx architecture on Au surface. Thus, in a first stage, B and PFe_3Mo_9 were successively deposited on the Au/MPS interface in order to obtain the Au/MPS/(B/PFe_3Mo_9)$_n$ multilayer structure. The monotonous increase of the steady-state SPR signal with the number of layers (n) (Fig. 2a) proves, without any doubt, that the immersion growth technique is useful to built up a multilayer structure containing up to 10 succesive layers of (B/PFe_3Mo_9).

Further, in order to obtain more information about the structure of the modified electrodes used for electrochemical measurements, the SPR signal was continuously monitored at Au/MPS surface when the Au/MPS/B/PFe_3Mo_9/B/GOx architecture was built up. Thus, the increase of the steady state SPR signal, recorded after the injection of a new structure constituent, follows qualitatively the corresponding increase of the architecture complexity (Fig. 2b).

This feature confirms again the existence of an ordered structure on the Au chip surface. Additionally, it was noticed that the increase of the SPR signal (Δ, RU) induced by the polymer (B) deposition, measured during the successive phases of Au/MPS/B/PFe_3Mo_9/B/GOx architecture construction, was significantly higher when B was deposited on Au/MPS/B/PFe_3Mo_9 surface (Δ= 2,005.1 RU) than it was deposited on Au/MPS surface (Δ=1,334.2 RU). This behavior points out to stronger interactions between B and the adjacent layer of PFe_3Mo_9 than those between B and the MPS layer, probably because of a higher density of negative charges in the PFe_3Mo_9 layer than in MPS one. Obviously, this aspect

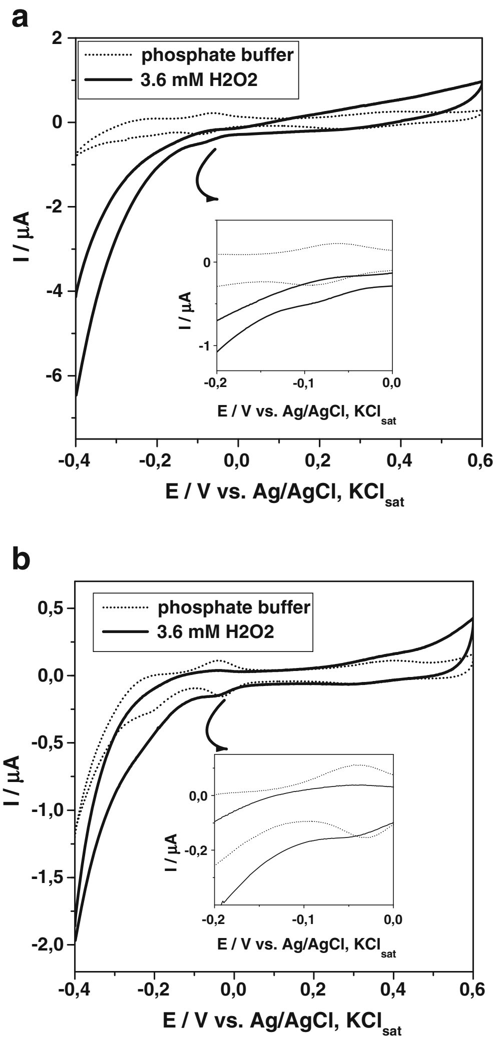

Fig. 4 Cyclic voltammograms showing the electrocatalytic effect for H_2O_2 electroreduction at Au/MPS/B/PFe_3Mo_9 (**a**) and Au/MPS/B/PFe_3Mo_9/B/GOx (**b**) modified electrodes. Experimental conditions: supporting electrolyte, 0.4 M Na_2SO_4 (pH 6.2); scan rate, 20 mV/s, starting potential, −0.4 V vs. Ag/AgCl,KCl$_{sat}$. The two insets show the potential windows useful for H_2O_2 amperometric detection

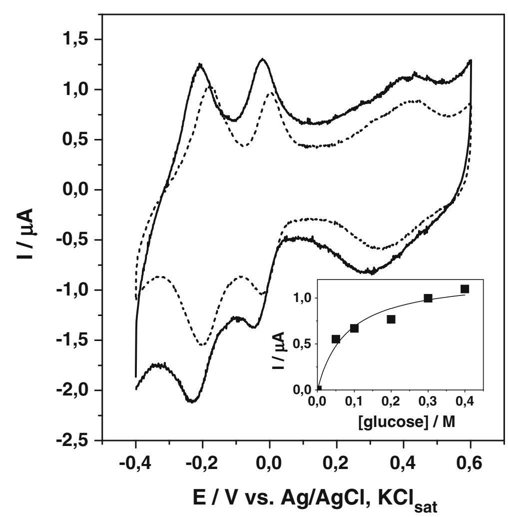

Fig. 5 Voltammetric response of Au/MPS/B/PFe_3Mo_9/B/GOx electrode observed in absence (*dot line*) and presence (*solid line*) of 50 mM glucose. Inset shows the calibration curve obtained from voltammetric data; $I_{p,c}$ stands for the cathodic current intensity of the peak I. Experimental conditions: supporting electrolyte, 0.4 M Na_2SO_4 (pH 6.2); scan rate, 100 mV/s, starting potential, −0.4 V vs. Ag/AgCl, KCl$_{sat}$

has a positive influence on the stability of the modified electrode.

Cyclic voltammetry performed at the Au/MPS/B/PFe_3Mo_9/B/GOx-modified electrode showed that the peak currents corresponding to the I–III waves (Fig. 3) depend linearly on the potential scan rate. Thus, the slopes of $\log I - \log v$ dependences, corresponding to I – III anodic peaks, were found 0.80 for peak I, 0.79 for peak II and 0.95 for peak III, proving once again that PFe_3Mo_9 layer is well immobilized into the multilayer structure. The discrepancy between the observed values and that expected for a surface confined redox couple (1) points out to a partial contribution of the diffusion to the charge transfer across the investigated structure.

Electrocatalytic behavior of modified electrodes based on PFe_3Mo_9

The well-known ability of Fe(III/II) couple to catalyze the H_2O_2 electroreduction was already reported for modified electrodes incorporating $PW_{11}O_{39}Fe(H_2O)^{4-}$ [5, 9] in polypyrrole [5] or in polyvinyl alcohol bearing styrylpyridinium groups [9]. Consequently, the new Au/MPS/B/PFe_3Mo_9 and Au/MPS/B/PFe_3Mo_9/B/GOx-modified electrodes were examined concerning their catalytic activity for H_2O_2 electroreduction. For this reason, cyclic voltammetric measurements were performed with both modified electrodes, in the absence and presence of H_2O_2 (Fig. 4). As it can be seen from Fig. 4a, b, both electrodes show a substantial electrocatalytic effect for H_2O_2 electroreduction. This effect is especially marked in the negative potential domain (see insets from Fig. 4), allowing the H_2O_2 determination in the optimal potential window for amperometric detection [38] Additionally, the comparison of the voltammetric responses of the investigated electrodes in presence of H_2O_2 (curves drawn with solid lines in Fig. 4a and b) revealed that the second structure was slightly less permeable to H_2O_2 than the first one, due to the inherent effect of GOx as diffusional barrier.

Irrespective of the type of the modified electrode, almost identical electrocatalytic efficiencies (estimated as the ratio between the catalytic currents in presence and in absence of H_2O_2, both currents were measured at the same potential, i.e., −0.1 V vs. Ag/AgCl,KCl_{sat}, situated between the standard potential values corresponding to the peak pairs I and II (Table 1)) were found: 191% for Au/MPS/B/PFe_3Mo_9 and 183% for Au/MPS/B/PFe_3Mo_9/B/GOx multilayer structure. These values were significantly higher than those already reported in literature: 17.4% for G/PVA/$PFeW_{11}$ and 5.5% for G/PPy/$PFeW_{11}$ (where PVA stays for poly (vinyl alcohol) and PPy stays for polypyrrole) [5].

The calibration of Au/MPS/B/PFe_3Mo_9 electrode for amperometric H_2O_2 detection was performed at an applied potential of −0.1 V vs. Ag/AgCl, KCl_{sat} under "batch" conditions (results not shown). The linear range up to 0.9 M and the sensitivity of (0.41±0.01 mA M^{-1}) (R^2=0.9962, n=9) were obtained. The response time, estimated as $t_{95\%}$, was less than 1 min.

Cyclic voltammetry measurements carried out at Au/MPS/B/PFe_3Mo_9/B/GOx evidenced a poor bioelectrocatalytic activity (Fig. 5). This can be the combined result of two effects: (i) the potential scan rate used to evidence the bioelectrocatalytic behavior was too high relative to the catalytic reaction rate; (ii) PFe_3Mo_9, used as mediator for H_2O_2 electroreduction, may oxidize directly GOx, competing with the natural co-substrate of the enzyme (O_2). The resulting effect of this side reaction will be the decrease of H_2O_2 production and, consequently, the attenuation of the expected bioelectrocatalytic activity for H_2O_2 electroreduction. The current intensity measured for the reduction peak I in presence of different glucose concentrations gave a calibration curve well obeying the Michaelis-Menten kinetics (inset Fig. 5). An apparent Michaelis-Menten constant (K_M^{app}) of 95 mM and a maximum current intensity (I_{max}) of 1.27 μA were estimated from the Lineweaver-Burk linearization.

The bioelectrode sensitivity (estimated as the I_{max}/K_M^{app} ratio) was 13.3 μA M^{-1} and the linear range was up to 50 mM. The response time necessary to reach 95% of the steady-state signal was found independent of the substrate concentration and its average value was less than 20 s. All these results prove that in the Au/MPS/B/PFe_3Mo_9/B/GOx-modified electrode, GOx is electrically well connected to the Au electrode via PFe_3Mo_9 mediator, both immobilized in an ordered multilayer structure based on electrostatic interactions.

Conclusions

Cyclic voltammetry corroborated with SPR measurements proved that exploiting electrostatic interactions and using the immersion growth variant of the layer-by-layer deposition method, a new multilayer ordered architecture incorporating PFe_3Mo_9 was successfully built up on Au surface.

Essentially, the electrochemical behavior of Au/MPS/B/PFe_3Mo_9-modified electrode maintains the redox characteristics of PFe_3Mo_9 complex previously observed at bare graphite electrode and naked Au electrode, too. Additionally, the new self-assembled modified electrode exhibits significant electrocatalytic activity towards H_2O_2 electroreduction. When GOx was deposited as the outermost layer on the Au/MPS/B/PFe_3Mo_9 electrode, a new bioelectrode, Au/MPS/B/PFe_3Mo_9/B/GOx for glucose amperometric detection was obtained.

In conclusion, by incorporating heteropolyoxometallates as electrocatalysts within simple and highly ordered three-dimensional architectures built up on electrostatic interactions, various self-assembled multilayer structures with desired electrochemical and electrocatalytical properties can be obtained. It was showed that a multilayer structure, incorporating PFe_3Mo_9 as electrocatalyst, is a versatile and reliable approach to obtain electrochemical interfaces, working as sensitive and selective transducers for amperometric sensors and biosensors.

Acknowledgments Authors gratefully acknowledge the financial support of CNCSIS–UEFISCSU (project PNII-ID-PCCE-129/2008).

References

1. Vuillaume PY, Mokrini A, Siu A, Theberge K, Robitaille L (2009) Eur Poly J 45:1641–1651
2. Kulesza PJ, Karnicka K, Miecznikowski K, Chojak M, Kolary A, Barczuk PJ, Tsirlina G, Czerwinski W (2005) Electrochim Acta 50:5155–5162
3. Foster K, Bi L, McCornac T (2008) Electrochim Acta 54:868–875
4. Tang Z, Liu S, Wang E, Dong S (2000) Langmuir 16:4946–4952
5. Gaspar S, Muresan L, Patrut A, Popescu IC (1999) Anal Chim Acta 385:111–117
6. Toth JE, Melton DJ, Cabelli D, Bielski BHJ, Anson FC (1990) Inorg Chem 29:1952–1957
7. Toth JE, Anson FC (1989) J Am Chem Soc 111:2444–2451
8. Turdean G, Patrut A, David L, Popescu IC (2009) J Appl Electrochem 38:751–758
9. Rong C, Anson FC (1996) Inorg Chim Acta 242–243:11–16
10. McCormac T, Fabre B, Bidan G (1997) J Electroanal Chem 425:49–54
11. Dong S, Liu M (1994) J Electroanal Chem 372:95–100
12. Keita B, Nadjo L (2007) J Mol Catal A 262:190–215
13. Song W, Wang X, Liu Y, Liu J, Xu H (1999) J Electroanal Chem 476:85–89
14. Skunik M, Kulesza PJ (2009) Anal Chim Acta 631:153–160
15. Dong S, Wang B (1992) Electrochim Acta 37:11–16
16. Cheng L, Niu L, Gong J, Dong S (1999) Chem Mater 11:1465–1475
17. Keita B, Bouaziz D, Nadjo L, Deronzier A (1990) J Electroanal Chem 279:187–203
18. Rajesh, Ahuja T, Kumar D (2009) Sensor Actuator B 136:275–286
19. Cheng L, Dong S (2000) J Electroanal Chem 481:168–176
20. Cheng L, Dong S (1999) Electrochem Commun 1:159–162
21. Liu S, Tang Z, Bo A, Wang E, Dong S (1998) J Electroanal Chem 458:87–97
22. Wang Y, Hu C (2005) Thin Solid Films 476:84–91
23. Gao S, Cao R, Li X (2006) Thin Solid Films 500:283–288
24. Mandler D, Turyan I (1996) Electroanal 8:207–213
25. Ammam M, Keita B, Nadjo L, Fransaer J (2010) Talanta 80:2132–2140
26. Decher G, Hong JD, Schmitt J (1992) Thin Solid Films 210/211:831–835
27. Lvov Y, Ariga K, Ichinose I, Kunitake T (1995) J Am Chem Soc 117:6117–6123
28. Laurent D, Schlenoff JB (1997) Langmuir 13:1552–1557
29. Caruso F, Niikura K, Furlong DN, Okahata Y (1997) Langmuir 13:3422–3426
30. Caruso F, Niikura K, Furlong DN, Okahata Y (1997) Langmuir 13:3427–3433
31. Laviron E (1979) J Electroanal Chem 101:19–28
32. Honeychurch MJ, Rechnitz GA (1998) Electroanal 10:285–293
33. Laviron E, Roullier L (1980) J Electroanal Chem 115:65–74
34. Zhang S, Berguiga L, Elezgaray J, Roland T, Faivre-Moskalenko C, Argoul F (2007) Surf Sci 601:5445–5458
35. Dostalek J, Homola J (2008) Sensor Actuator B 129:303–310
36. Keith Roper D (2007) Chem Eng Sci 62:1988–1996
37. Chien F-C, Chen S-J (2004) Biosens Bioelectron 20:633–642
38. Gorton L (1995) Electroanal 7:23–45